RECENT APPLICATIONS OF PLASTICITY THEORY TO CONCRETE SHEAR PROBLEMS

Tim IBELL [1] Steve DENTON [2]

[1] Department of Architecture and Civil Engineering, University of Bath, UK
[2] Parsons Brinckerhoff, UK

Keywords: anchorage, confinement, concrete, ductility, plasticity, prestressing, shear, strengthening

1 INTRODUCTION

This paper summarises various research projects which have been published by the authors over the past five years. The underlying theme across all projects is the use of plasticity theory to help in the explanation of structural behaviour, and it is this specific theme, in particular, which is presented here for each project. The various aspects which this paper touches on are:

- Fibre-Reinforced Polymer (FRP) reinforced and prestressed concrete beams
- Anchorage zones for non-metallic prestressed concrete structures
- Shear assessment of bridge decks containing inadequately-anchored reinforcement
- Shear assessment and strengthening of laterally-prestressed concrete bridges

2 FRP REINFORCED AND PRESTRESSED CONCRETE BEAMS

This project was funded by the EPSRC and was carried out to study ductility and shear capacity in helically-FRP-reinforced concrete beams [1]. An FRP helix placed in the compression zone of a concrete beam greatly enhances bending capacity and ductility [2]. But the question was what effect this helix might have on the shear behaviour. Figure 1 shows the layout of various helical (both circular and rectangular) reinforcement regimes which were studied, while Figure 2 shows a photograph of a typical cage which was constructed.

Figure 3 shows the analytical model which was used to study shear collapse of the resulting specimens. By using experimentally-obtained bond-slip relations for the FRP materials, and by adopting the Mohr Coulomb Failure Criterion for the concrete, the problem became one of determining the level of shear force which the failure mechanism could endure prior to failure.

Figure 4(a) shows the Modified Coulomb Failure Criterion and three Mohr's Circles. The failure criterion is defined in terms of the uniaxial compressive strength, f_c, of the concrete (dashed line circle) in that it just touches the failure surface. What is required is to determine what level of shear stress, τ, may be added to some original uniaxial compressive stress state (solid line circle, of radius $\frac{1}{2}\alpha f_c$) to develop a critical stress state Mohr's circle for sliding failure (dot-dashed line circle) of radius $\sqrt{(\frac{1}{2}\alpha f_c)^2 + \tau^2}$. By developing a relationship between α and τ, it is possible to determine by how much f_c should be reduced (factored by α) to allow for co-existing shear stress at the critical state.

For sliding failure,

$$\tau = \sigma\tan\varphi + c \tag{1}$$

Then, from the geometry shown in Figure 4(b),

$$c + \tfrac{1}{2} f_c(1 - \sin\varphi)\tan\varphi = \tfrac{1}{2} f_c\cos\varphi \tag{2}$$

Therefore,

$$c = \tfrac{1}{2} f_c\left(\frac{1-\sin\varphi}{\cos\varphi}\right) \tag{3}$$

Now, as can be seen from Figure 4(c),

$$d = \tfrac{1}{2}\alpha f_c - \left(\sqrt{(\tfrac{1}{2}\alpha f_c)^2 + \tau^2}\right)\sin\varphi \tag{4}$$

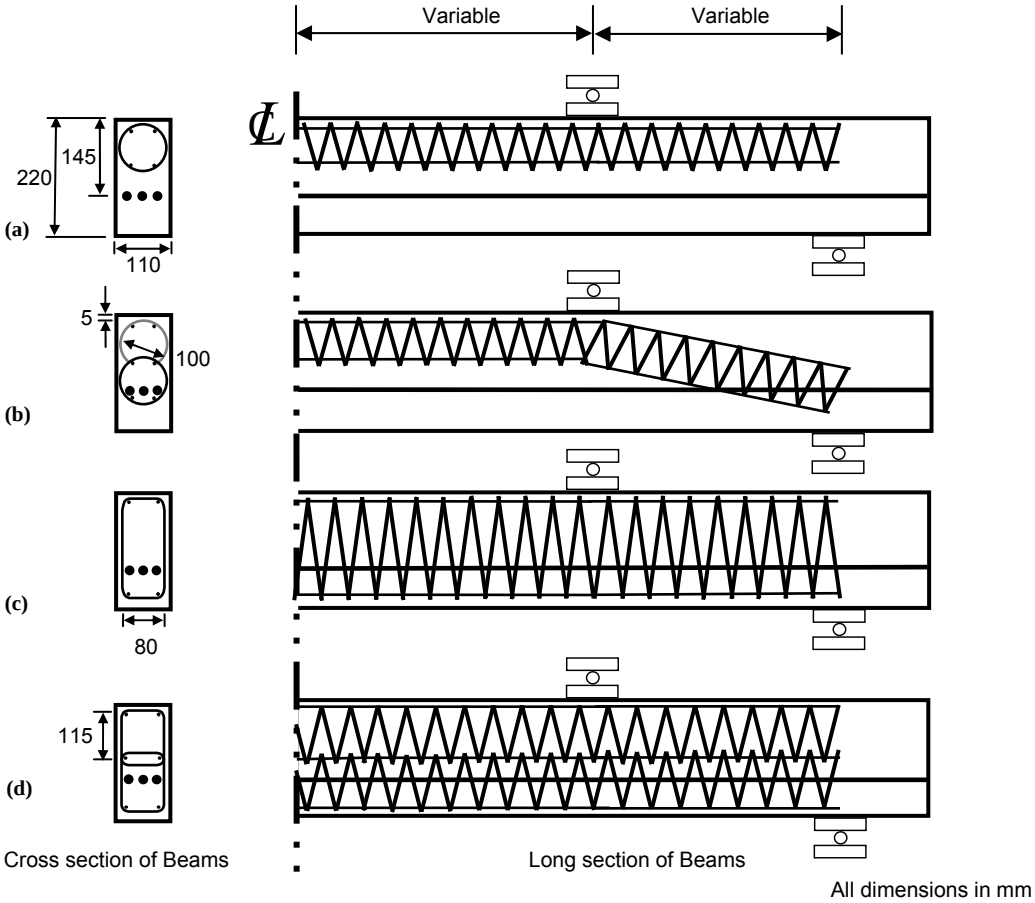

Fig. 1 Cross-sectional dimensions and helical reinforcement shapes for (a) Specimens containing a circular helix placed along the top of the beam, (b) Specimens containing a circular helix angled in the shear zone, (c) Specimens containing a continuous draped rectangular helix, and (d) A specimen containing two interlocking rectangular helices.

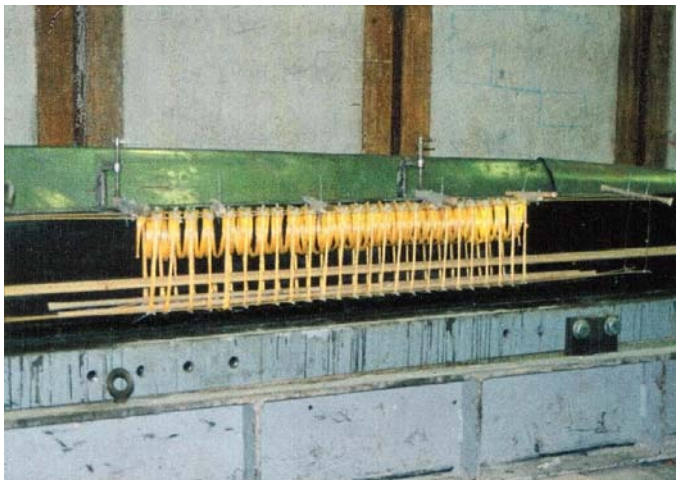

Fig. 2 Typical cage detail for the specimens.

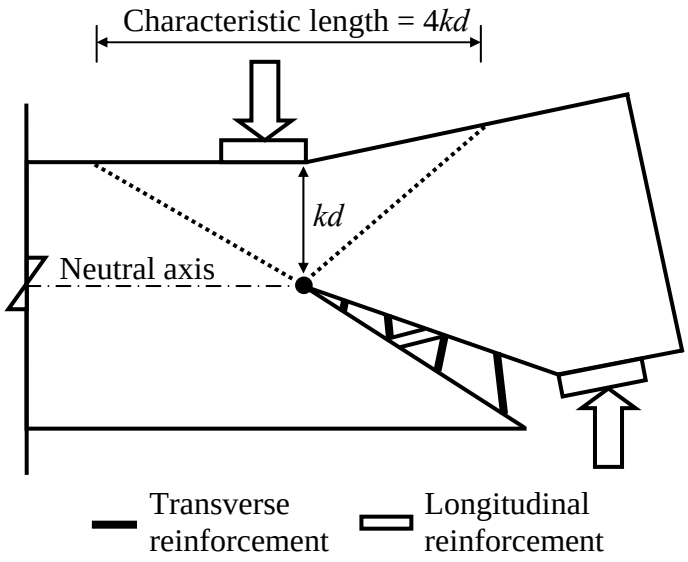

Fig. 3 Assumed rigid-body rotation shear model.

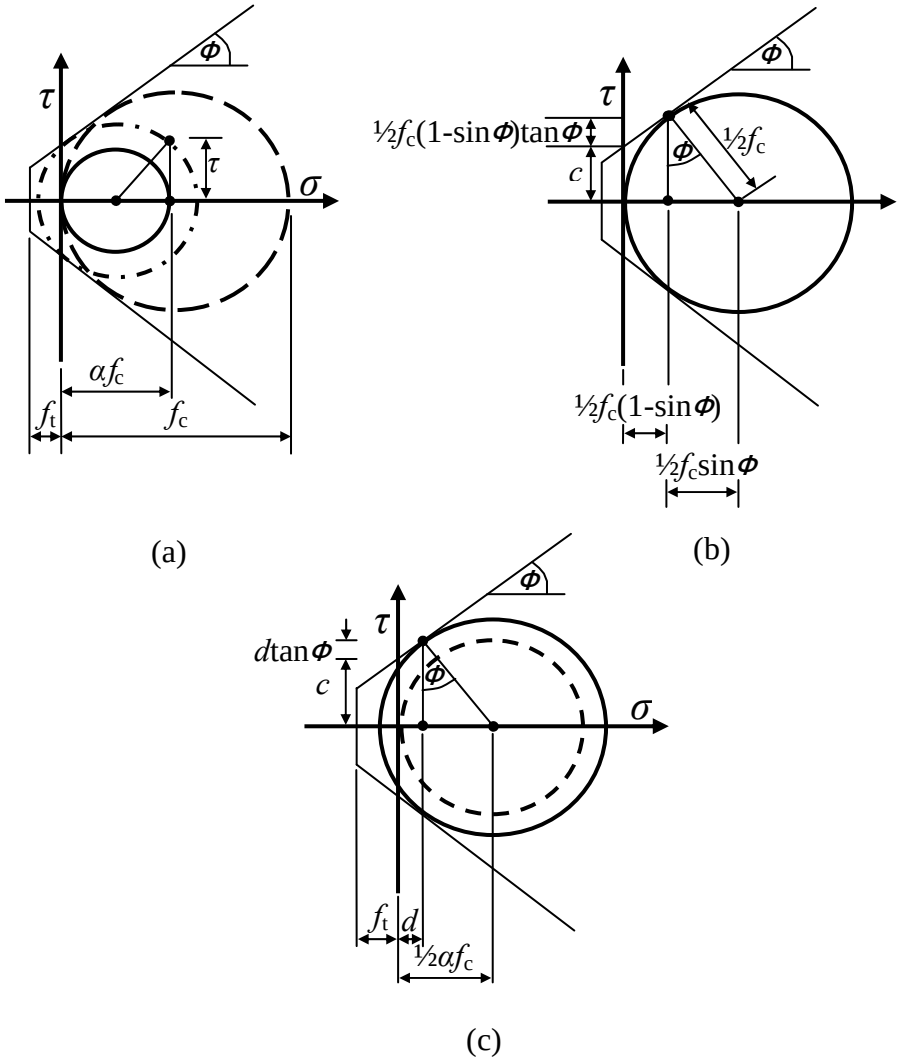

Fig. 4 (a), (b) and (c) Mohr's circles of stress for consideration of sliding failure.

and

$$d\tan\varphi + c = \left(\sqrt{(½\alpha f_c)^2 + \tau^2}\right)\cos\varphi \tag{5}$$

Substitution of (3) and (4) into (5) yields

$$\left(½\alpha f_c - \left(\sqrt{(½\alpha f_c)^2 + \tau^2}\right)\sin\varphi\right)\tan\varphi + ½ f_c\left(\frac{1-\sin\varphi}{\cos\varphi}\right) = \left(\sqrt{(½\alpha f_c)^2 + \tau^2}\right)\cos\varphi \tag{6}$$

This provides the required relationship between α and τ. Rearranging (6), it is found that

$$\frac{\tau^2}{(½f_c)^2} = (\sin^2\varphi - 1)\alpha^2 - 2\sin\varphi\,(\sin\varphi - 1)\alpha + (1-\sin\varphi)^2 \tag{7}$$

Finally, solving equation (7) for τ provides

$$\tau = ½f_c\sqrt{(\sin^2\varphi - 1)\alpha^2 - 2\sin\varphi(\sin\varphi - 1)\alpha + (1-\sin\varphi)^2} \tag{8}$$

Alternatively, solving equation (7) for the positive root of α provides

$$\alpha = \frac{2\sin\varphi\,(\sin\varphi - 1) - \sqrt{4\sin^2\varphi\,(\sin\varphi - 1)^2 - 4(\sin^2\varphi - 1)\left((1-\sin\varphi)^2 - \frac{\tau^2}{(½f_c)^2}\right)}}{2(\sin^2\varphi - 1)} \tag{9}$$

Although Figure 4(c) is drawn to show sliding failure, rather than separation failure, it can be seen that the following relationship exists at separation failure:

$$½\alpha f_c - \sqrt{(½\alpha f_c)^2 + \tau^2} = -f_t \tag{10}$$

Re-arranging,

$$\tau = \sqrt{(½\alpha f_c + f_t)^2 - (½\alpha f_c)^2} \tag{11}$$

And on re-arranging equation (11) to solve for α, it is found that

$$\alpha = \frac{\tau^2 - f_t^2}{f_c . f_t} \tag{12}$$

Figure 5 shows the variation in the theoretical value of α (the proportion of uniaxial compressive strength, f_c) versus the co-existing applied shear stress for the confined specimens, according to each of the two failure criteria above (equations (9) and (12)). Also shown in Figure 5 are 'safe' and 'unsafe' regions of combinations of α and τ. In order to create this figure using specific values, a series of preliminary tests on cylindrical specimens confined with AFRP helices was conducted.

The tests had shown that the helices were stretched considerably, as shown in Figure 6, signifying considerable confining behaviour. Predictions for shear strength were carried out using the model above, and Figure 7 contains comparisons between predictions and actual results for three markedly different beam types. Note that the predicted plots were based on an initial elastic stiffness prediction, followed by a plastic-based approach described above in which the concrete behaviour was considered to be fully plastic and the reinforcement behaviour was assumed to be dependent on predetermined bond-slip relationships. Correlation was generally good. This work was subsequently extended into heavily over-reinforced situations [3], which demonstrated that the use of a helix in over-reinforced beams is extremely beneficial, and this behaviour was found again to be predictable.

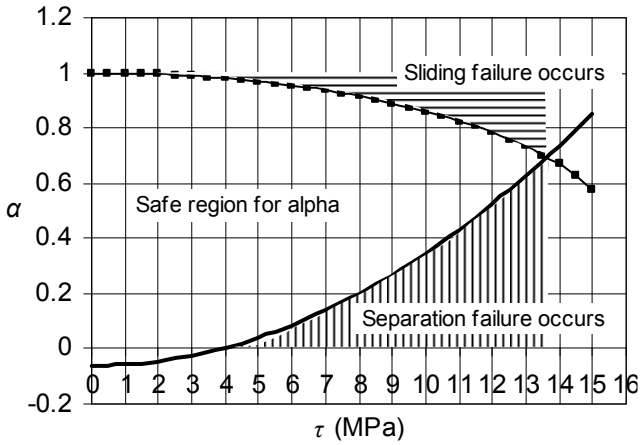

Fig. 5 Variation in the theoretical value of α versus the applied shear stress, according to each of the two failure criteria.

Fig. 6 Rupture of confining helix in the constant moment region of specimen.

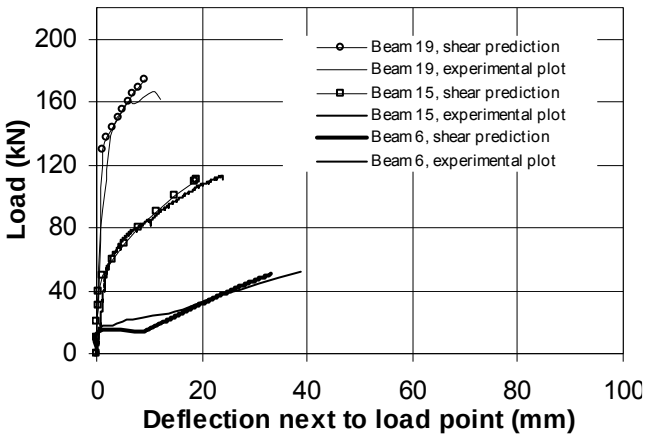

Fig. 7 Load-deflection response for three beams.

3 ANCHORAGE ZONES FOR NON-METALLIC PRESTRESSED CONCRETE STRUCTURES

This project was funded by the EPSRC and carried out to study ductility and capacity of anchorage zones in FRP-prestressed concrete beams containing FRP reinforcement. Both primary zones and secondary zones were studied [4,5].

3.1 Primary zones

Through carrying out various tests, it was discovered that the form of FRP reinforcement in primary anchorage zones which provided the greatest capacity and best ductility response for a given quantity of reinforcement was that shown in Figure 8. What is needed in primary zones seems to be a double helix system local to the concentrated load (to confine the pathway of the advancing cone of concrete), and a co-existent mat of FRP reinforcement to directly resist the slightly deeper bursting tensile stress resultant.

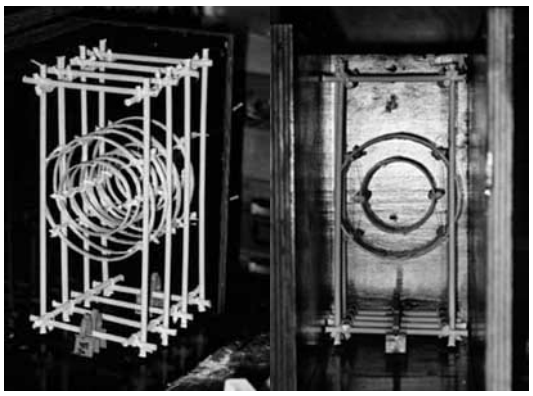

Fig. 8 Combined mat and helix system for primary zone reinforcement.

A lower-bound plasticity approach was adopted for this problem, as shown in Figure 9, in which the concrete was assumed to be fully plastic and the reinforcement was assumed to obey a bond-slip relationship which had been discovered previously [4]. The following equation was derived for the value of the normal stress along the failing plane in the concrete.

$$\sigma = \frac{a \cdot c_c A \cos\beta - a_1 c_c A \cos\beta + 2c_c HA \sin\beta + 8T_T \left[H - \left(15 - H_r/2\right)\right]}{a_1 A \tan\phi \cos\beta - aA \tan\phi \cos\beta - aA \sin\beta + a_1 A \sin\beta + 2HA \cos\beta - 2HA \sin\beta \tan\phi} \quad (13)$$

By allowing the height of the prism to approach infinite dimensions, so that a long beam could be considered, the following simplified equation for the stress may be obtained.

$$\sigma = \frac{c_c A \cos\beta + 4T_T}{A\left(\cos\beta - \sin\beta \tan\phi\right)} \quad (14)$$

Figure 10 shows a few predictions which were found for the overall behaviour of such specimens. Note that although the plasticity model predicts significant capacity at zero displacement, these plots may easily be generalised to include an initial elastic response, which would then create a fully elasto-plastic behavioural prediction. The predictions were considered to be reasonably accurate, and the experimental results themselves demonstrated clearly that some ductility is certainly possible to be extracted from FRP-reinforced anchorage zones as long as careful thought is given to the positioning of the bars.

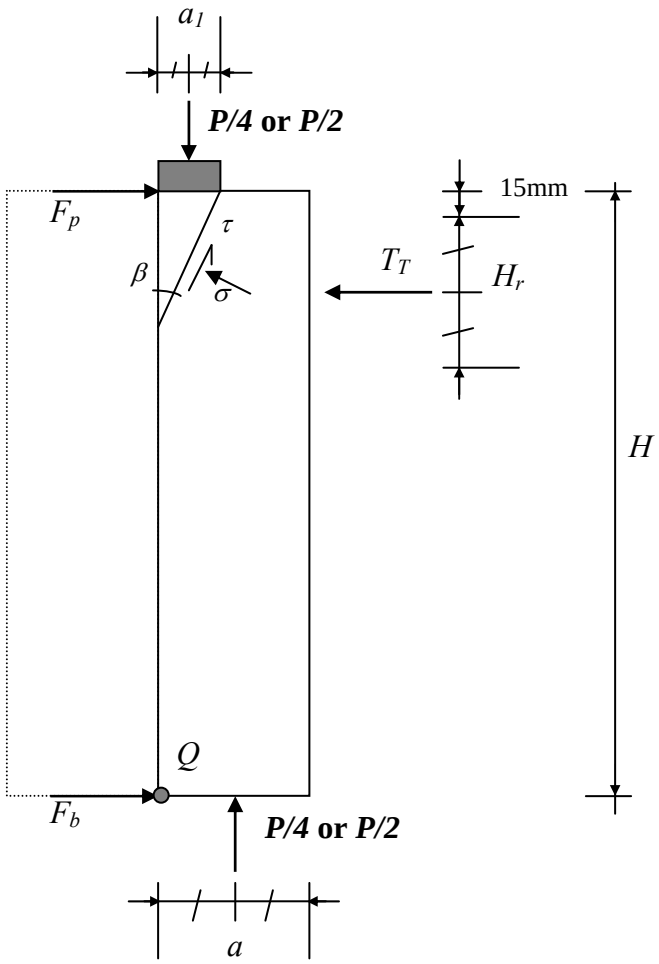

Fig. 9 Lower-bound equilibrium model of failure.

3.2 Secondary zones

Secondary zones in end blocks are an important consideration in design, as they reflect interaction amongst the several primary zones. Figure 11 shows the two main types of secondary zones which are encountered (and which were tested), namely 'Zone A' and 'Zone B', representing remotely-spaced and closely-spaced primary zones, respectively.

What was discovered during the tests on secondary zones was that the final failure mechanism was always primary in nature, ie failure occurred under one or more of the loading plates, rather than being more 'secondary' in nature. Therefore, initially two mechanisms to model this behaviour were considered, as shown in Figure 12. The predictions from these mechanisms, using a similar approach to that adopted above for the primary zones but with some significant amendments, proved to be on the low side. By studying the failure mechanisms a little more closely, it became clear that the failure wedges beneath the loading plates were, in fact, bulging in shape, as shown in Figure 13. By developing a 2-dimensional Airy stress function approach to this problem, it was found that indeed the areas just adjacent to the loading plates were in fact in compression for a small distance laterally. Where this compression turned to tension was considered to be the extent of the 'real' cone moving into the concrete, as shown schematically in Figures 13 and 14. By considering this new dimension for the cone, predictions against reality were found to be fairly accurate, and four representative predicted vs actual load-deflection plots are shown in Figure 15, in which the elastic portion of the plot is predicted using the Airy stress function approach and the plastic portion is predicted based on a similar procedure to that described above for the primary zones.

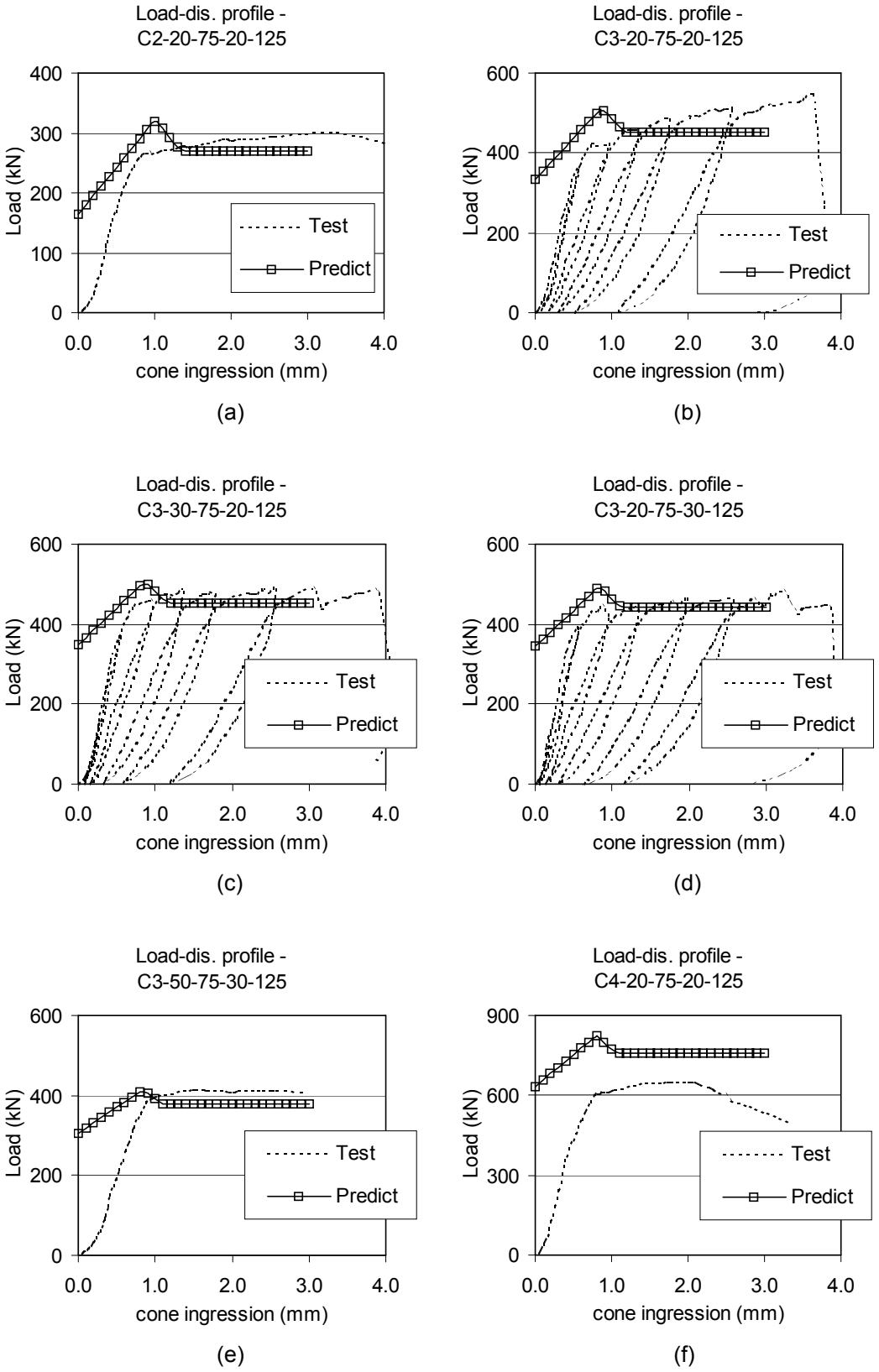

Fig. 10 Analytical load-displacement profiles for double helix cylindrical specimens.

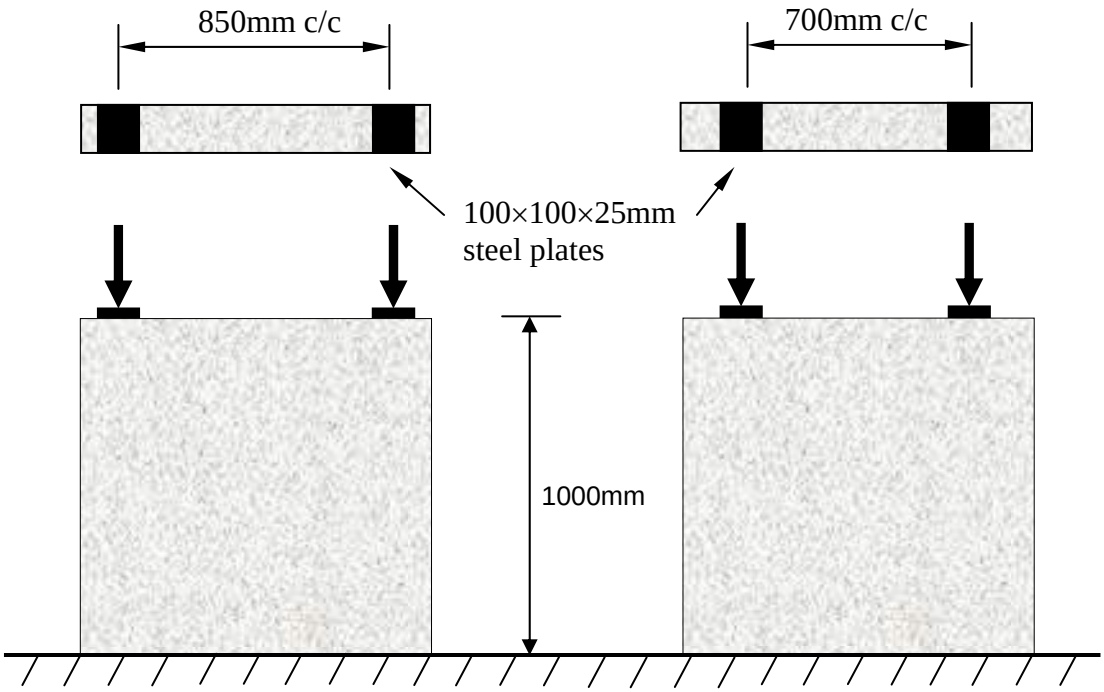

(a) Zone A specimens

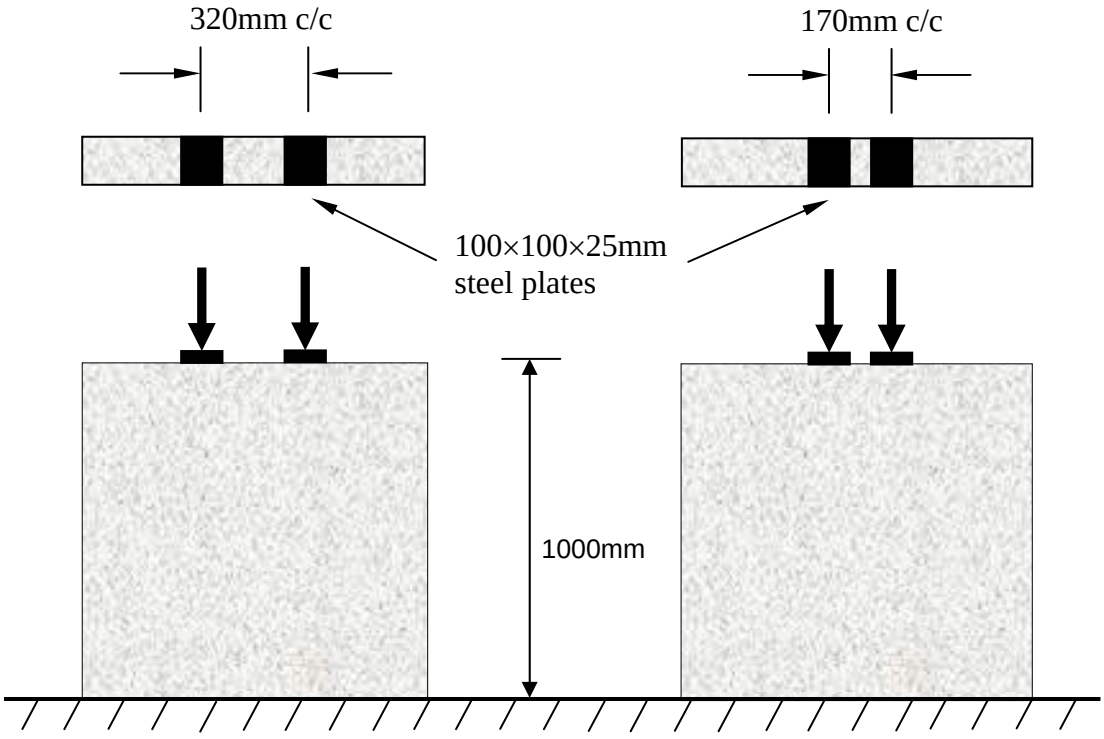

(b) Zone B specimens

Fig. 11 Loading arrangements for Zones A and B test series.

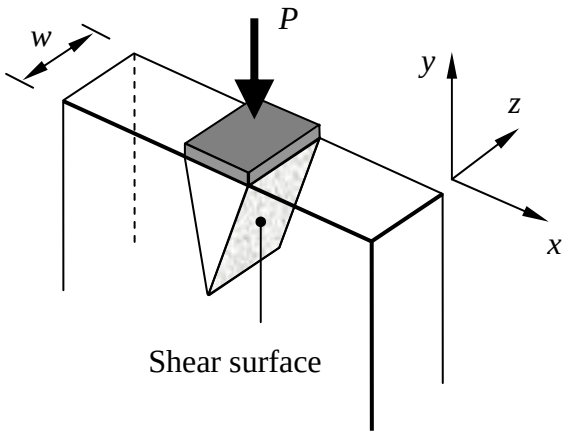

(a) Two-dimensional failure surface

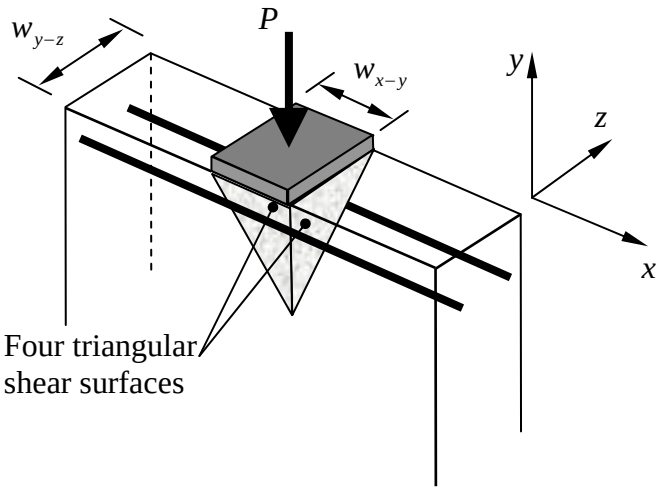

(b) Three-dimensional failure surface

Fig.12 Isometric illustration of 2- and 3-dimensional wedging failures with secondary FRP bar reinforcement present.

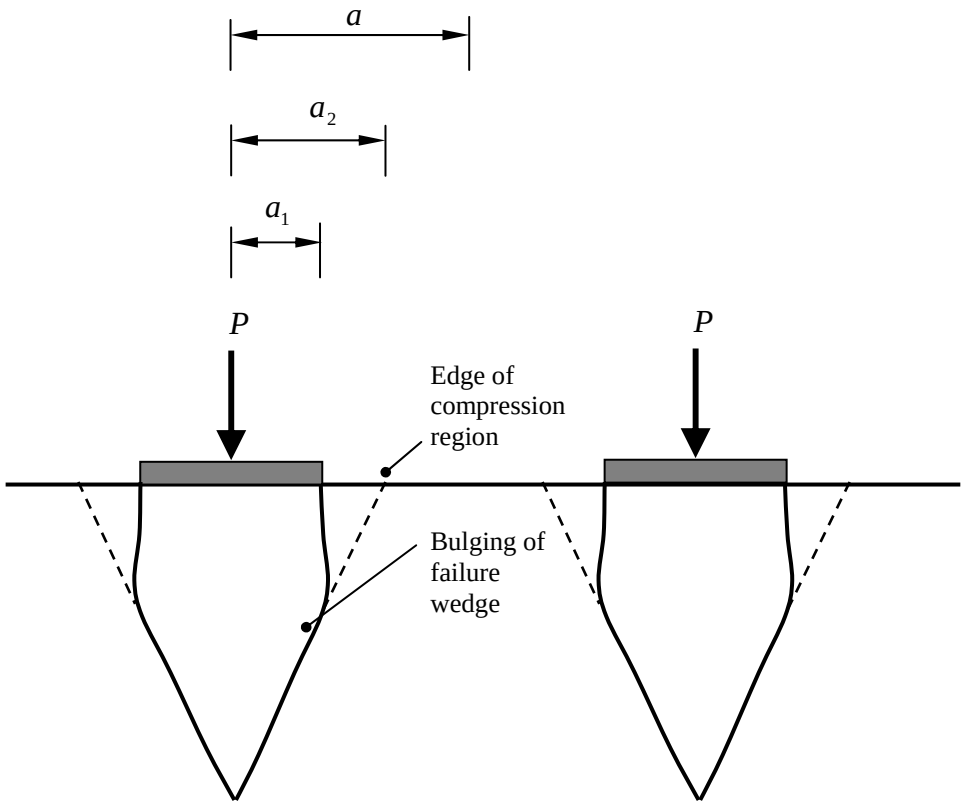

Fig. 13 Simplified shape of wedge bulging, taken to edge of compression region.

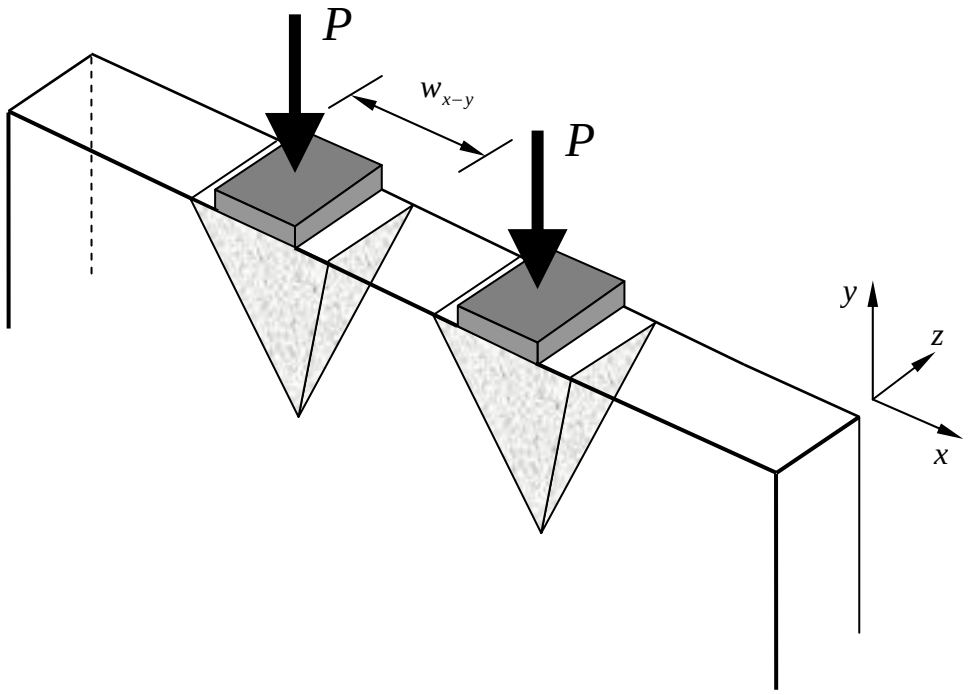

Fig. 14 Isometric illustration of 3-dimensional wedging beneath both loading plates emanating from the edges of the compression region.

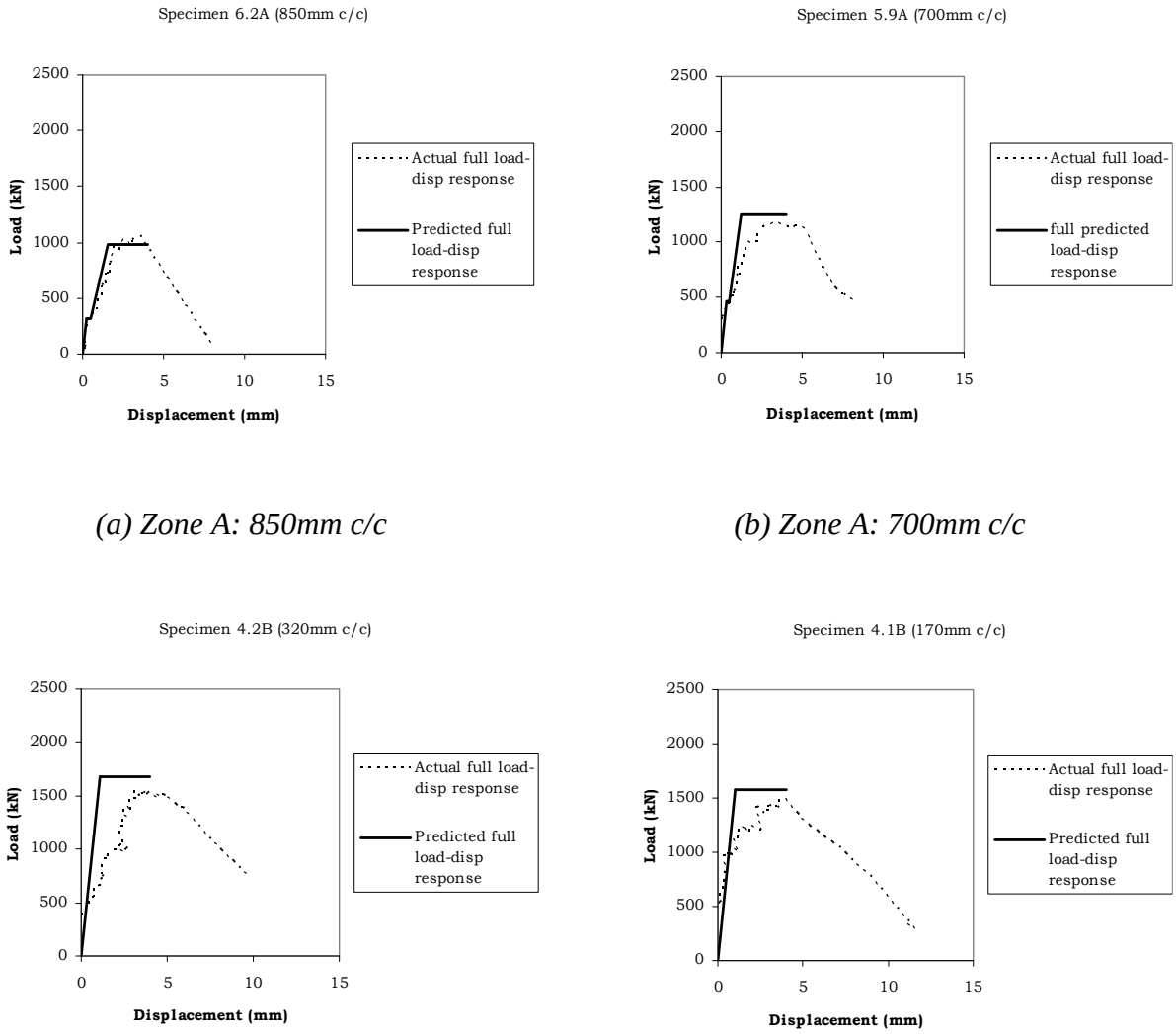

(a) Zone A: 850mm c/c

(b) Zone A: 700mm c/c

(c) Zone B: 320mm c/c

(d) Zone B: 170mm c/c

Fig. 15 Comparison of actual versus predicted load-displacement plot for each loading arrangement.

4 SHEAR ASSESSMENT OF BRIDGE DECKS CONTAINING INADEQUATELY-ANCHORED REINFORCEMENT

It had been known for many years that there existed anomalies in BD44/95 [6] concerning shear capacity of concrete bridges when the steel reinforcement is curtailed. The neglect of shear enhancement near to supports, the neglect of stirrup contribution in the presence of poorly-anchored longitudinal reinforcement, the use of bar diameters to judge anchorage rather than bond itself and the neglect of type of reinforcing steel (smooth or deformed) all caused concern to the profession. This EPSRC-funded project aimed to study this problem rationally [7].

A total of 72 tests on slab specimens, such as that shown in Figure 16, were conducted. Each test involved loading the specimen at five locations between *d* and *3d*, at ever-increasing load levels, so that there could be assurance of proof-loading at all possible critical positions. Final loading to failure occurred at various shear spans across all 72 tests. The fundamental finding was that the present BD44/95 clause for shear capacity of concrete bridge decks containing inadequately-anchored reinforcement is unduly conservative.

Fig. 16 Typical slab specimen test set-up.

By carrying out upper- and lower-bound plasticity-based analyses, as shown in Figures 17 and 18, a rational approach to the problem was developed. Predictions from the lower-bound approach provided correlation with the test data as shown in Figure 19. This figure should be compared with Figure 20, which shows correlation between the predictions of BD44/95 and the test data. Clearly, there is significant improvement. The clause extract shown in Figure 21 is proposed for the new BD44/95 approach to shear capacity under such conditions of inadequate anchorage.

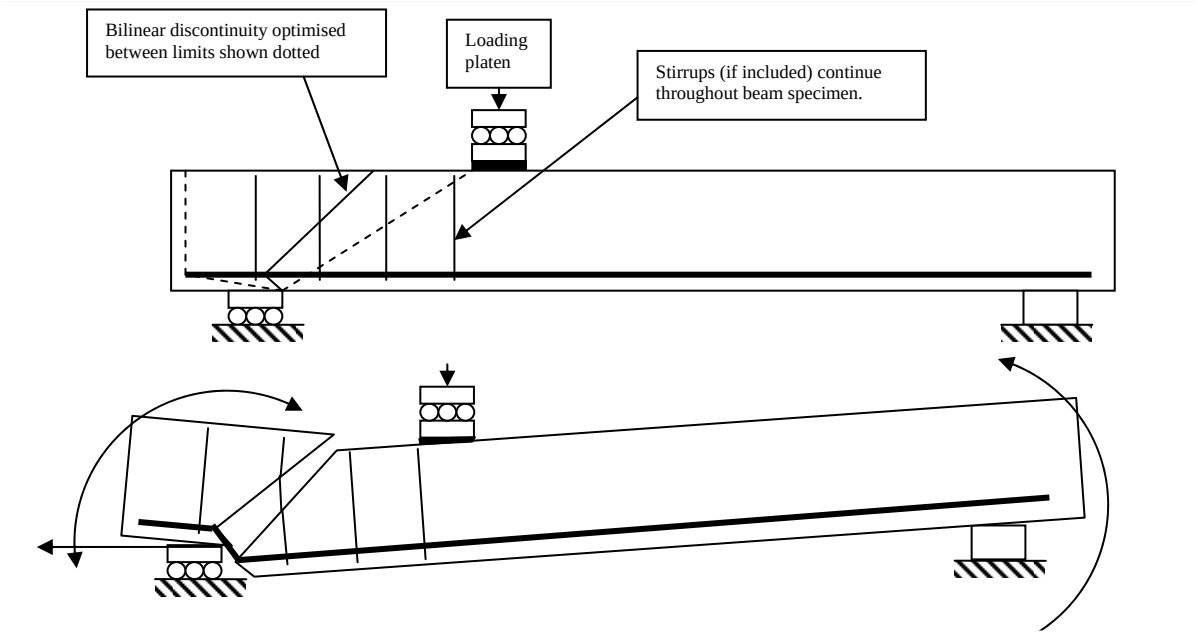

Fig. 17 Upper bound model with bilinear discontinuity.

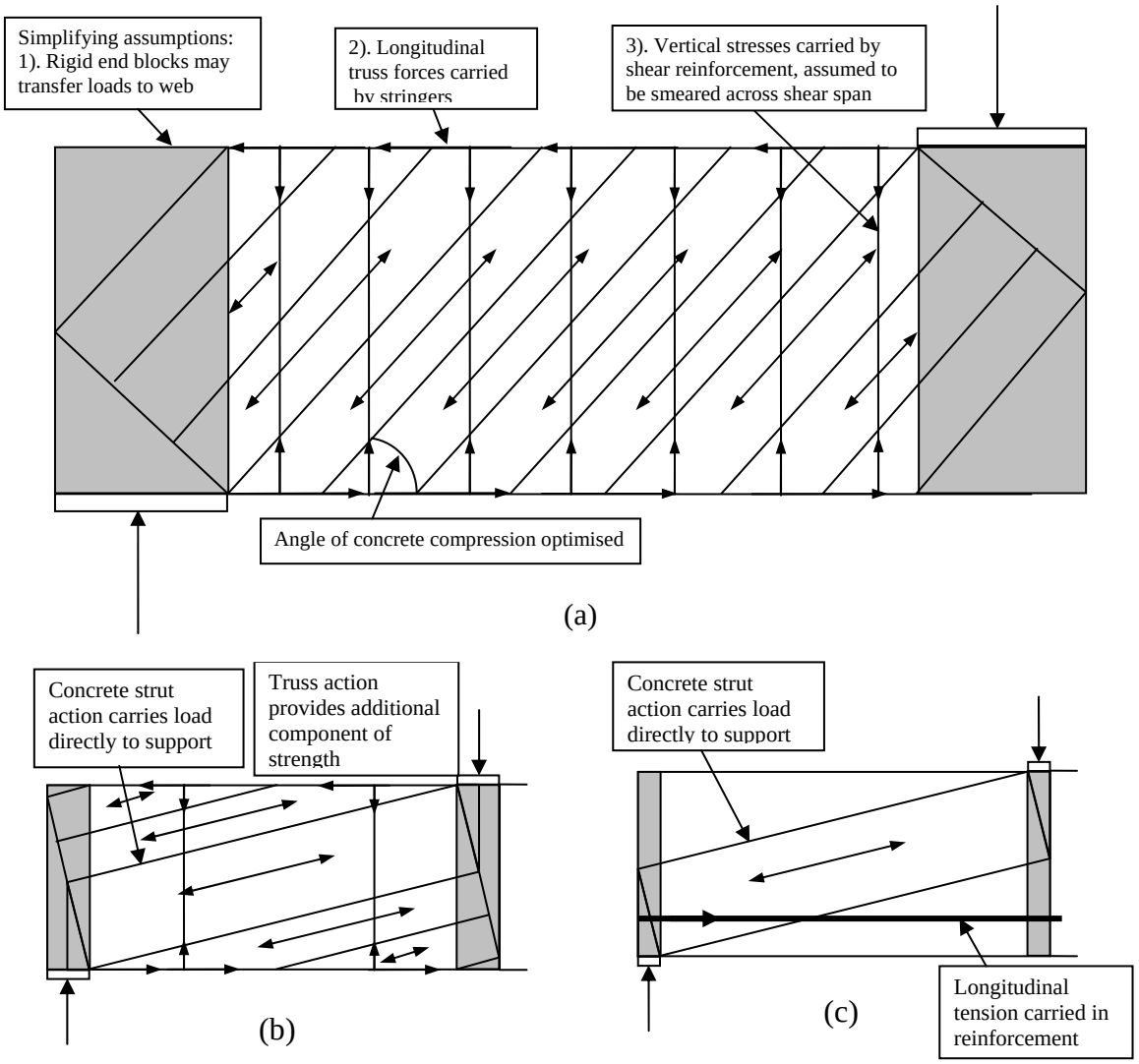

Fig. 18 Lower-bound models: (a) Variable angle truss action, (b) Combined strut and truss action, (c) Strut action.

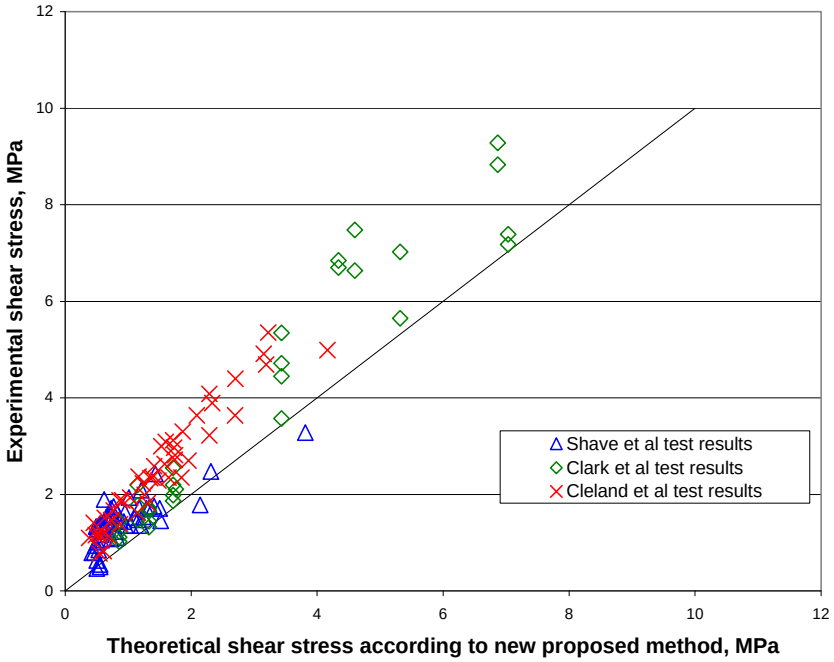

Fig. 19 Correlation of proposed method with test data.

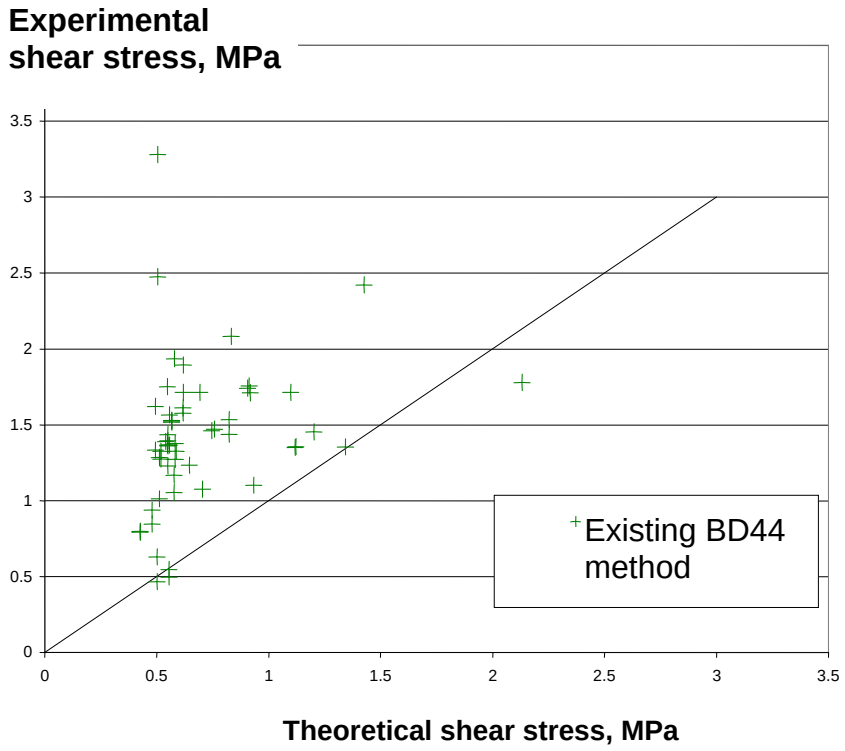

Fig. 20 Correlation of BD44/95 with test data.

In the absence of effective shear reinforcement, the ultimate shear resistance, V_u, of a section is given by

$$V_u = \Gamma \kappa \xi_s v_c b_w d$$

Where effective vertical links are present the ultimate shear resistance V_u of a section shall be taken as

$$V_u = \Gamma \left(\kappa \xi_s v_c b_w d + \frac{f_{yv}}{\gamma_{ms}} \frac{d}{s_v} A_{sv} \right)$$

V_u should not be taken as less than $\xi_s \frac{0.24}{\gamma_{mv}} \left(0.15 f_{cu}\right)^{1/3} b_w d$.

is a reduction factor to allow for inadequate anchorage of the longitudinal reinforcement, and shall be calculated as follows:

$\Gamma = \sqrt{\frac{F_{ub}}{F_{ub\max}}}$ but not greater than unity.

where

F_{ub} is the total ultimate anchorage force in the tension reinforcement at the front face of the support as calculated in 5.8.6.3, but not greater than $A_s f_y / \gamma_{ms}$

and

$$F_{ub\max} = 3 \xi_s v_c b_w d$$

Fig. 21 Proposed new clause for BD44/95.

5 SHEAR ASSESSMENT AND STRENGTHENING OF LATERALLY-PRESTRESSED CONCRETE BRIDGES

This EPSRC-funded project looked at the issue of shear assessment of existing laterally-prestressed concrete bridges, particularly in Network Rail's stock [8]. There are hundreds of rail bridges across the UK which consist of longitudinal rectangular prestressed concrete beams, laterally post-tensioned together to create a 'plate' system. The issue was that these bridges were routinely failing analytical shear assessments, and a rational approach to their consideration was needed. Further, should it prove necessary to strengthen them, a practical, cost-effective strengthening strategy was sought. This project produced solutions to both questions. Figure 22 shows the test set-up which was used to study the problem. Fundamentally, the tests showed a tremendous amount of redistribution of stress within the system due to the lateral prestress, and demonstrated that even under only 25% of the credible lateral prestress, the system was still safe under fully factored loading. By applying suitable upper- and lower-bound solutions to the problem, correlation between predictions and test data was reasonably good, as shown in Figure 23.

Even though the testing demonstrated that the bridges under scrutiny on the Network Rail stock were safe, and that their shear capacity was predictable, a novel shear-strengthening system was investigated for such bridges, namely the deep embedment system, developed previously at the University of Bath [9]. It consists of drilling holes upwards from the soffit, and resining in either steel or FRP bars. This system negates any top-surface preparation and means that access to the webs of each beam is unnecessary. Figure 24 demonstrates its implementation. This system was shown to be practical and even more effective than the equivalent near-surface mounted (NSM) strengthening scheme due to there being no possibility of cover spalling.

Fig. 22 Laterally-prestressed concrete bridge deck under load.

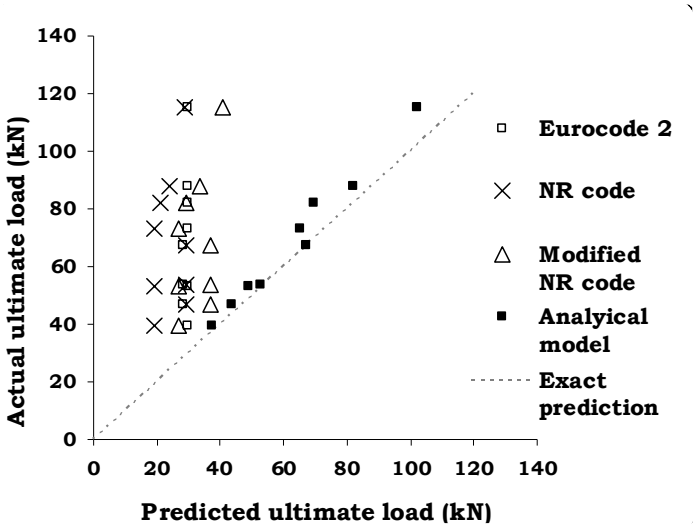

Fig. 23 Correlation between analytical model predictions and test data.

Fig. 24 Deep embedment shear strengthening technique.

The upper-bound approach was again used to predict strengthened capacity, and Figure 25 shows details of the various mechanisms which were investigated. In particular, bond-slip test data on the FRP bars was used in the analysis, and the required anchorage length at each end of each bar was considered when deciding on effectiveness of each bar in the model. Again, it was demonstrated that the predictions using this approach were reasonably accurate, so that Network Rail now has a rational analytical technique for assessment of its existing and its strengthened concrete bridges.

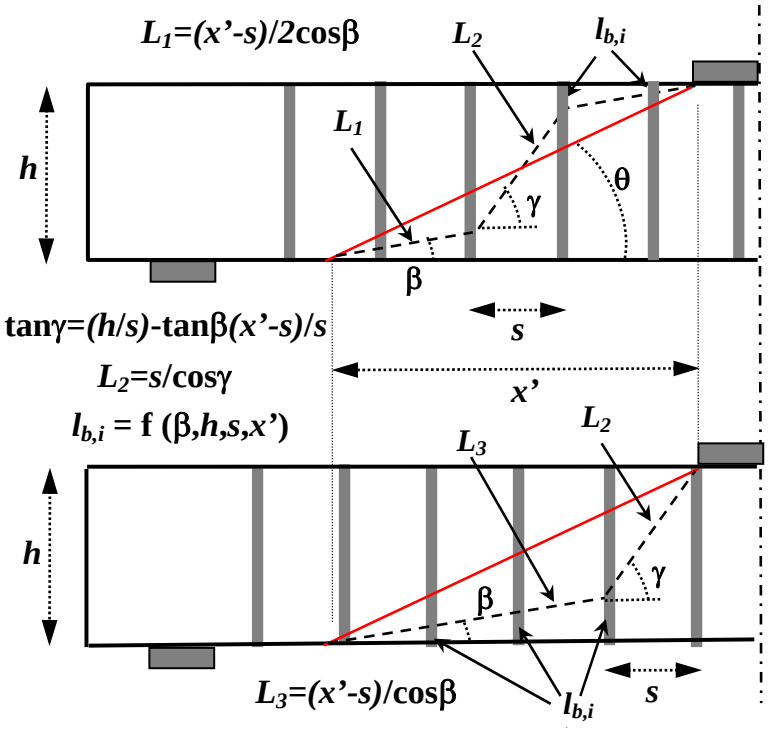

Fig. 25 Upper-bound mechanisms for the strengthened specimens.

6 CONCLUSIONS

There is little doubt that plasticity theory offers the analytical means to study shear problems in concrete in a rational manner, albeit under the exceptionally important caveat of ductility requirement. The examples referred to in this paper demonstrate the potential strength of plasticity, particularly in the field of structural assessment of existing concrete structures.

ACKNOWLEDGEMENTS

This work was carried out in very close collaboration with many other researchers. In alphabetical order, they are Dr Man-Cho Choi, Dr Antony Darby, Dr Luke Gale, Dr Jonathan Shave, Dr Pierfrancesco Valerio and Dr Paul Whitehead. Their contributions to the findings presented in this paper are profound. The laboratory staff at the University of Bath carried out the testing presented here, and thanks are due to them. Finally, without the support of the EPSRC, none of this work would have been conducted to the depth to which it was indeed possible.

REFERENCES

[1] Whitehead, P.A and Ibell, T.J. (2005) Rational approach to shear design in fibre-reinforced polymer-prestressed concrete structures, *ASCE Journal of Composites for Construction*, 9 (1), pp. 90-100.

[2] Burgoyne, C.J. (1997). Rational use of advanced composites in concrete, *Technical Report CUED/D-Struct/TR167*, Cambridge University Engineering Department.

[3] Whitehead, P.A. and Ibell, T.J. (2004) Deformability and ductility in over-reinforced concrete structures, *Magazine of Concrete Research*, 56, (3), April, pp. 167-178.

[4] Choi, M.C. and Ibell, T.J. (2004) Behavior of fiber-reinforced polymer reinforced anchorage zones for post-tensioned concrete structures, *ACI Structural Journal*, 101, (5), September, pp. 625-632.

[5] Gale, L. and Ibell, T.J. (2005) Multiple anchorage zones in fibre-reinforced polymer prestressed concrete structures, *Magazine of Concrete Research*, 57 (3), April, pp. 149-166.

[6] BD44/95 (1995) The Assessment of Concrete Highway Bridges and Structures, *Highways Agency*, HMSO, London.

[7] Shave, J.D., Ibell T.J. and Denton, S.R. (2007) Shear assessment of reinforced concrete bridges with short anchorage lengths, *The Structural Engineer*, 85 (5). pp. 30-37.

[8] Valerio, P., Ibell, T.J. and Darby, A.P. (2006) Shear strengthening of prestressed concrete bridges using embedded FRP bars, *Proceedings of the 2nd FIB Congress*, Federation Internationale du Beton, June, paper ID 10-71, Naples, Italy.

[9] Valerio, P. and Ibell, T.J. (2003). Shear strengthening of existing concrete bridges, *ICE Journal of Structures and Buildings*. 156 (1) pp. 75-84.